

Effect of oxygen-doping on $\text{Bi}_2\text{Sr}_2\text{Ca}_2\text{Cu}_3\text{O}_{10+\delta}$ vortex matter: Crossover from electromagnetic to Josephson interlayer coupling

A. Piriou,* Y. Fasano, E. Giannini, and Ø. Fischer

Département de Physique de la Matière Condensée, Université de Genève, 24 Quai Ernest-Ansermet, 1211 Geneva, Switzerland

(Received 18 February 2008; revised manuscript received 16 April 2008; published 13 May 2008)

We study the effect of oxygen-doping on the critical temperature T_c , the vortex matter phase diagram, and the nature of the coupling mechanism between the Cu-O layers in the three-layer $\text{Bi}_2\text{Sr}_2\text{Ca}_2\text{Cu}_3\text{O}_{10+\delta}$ (Bi-2223) compound. Contrary to previous reports, in the overdoped (OD) regime, we do find a variation in T_c by increasing the oxygen partial pressure of the postannealing treatment. This variation is less significant than in the bilayer compound $\text{Bi}_2\text{Sr}_2\text{CaCu}_2\text{O}_{10+\delta}$ (Bi-2212) and does not follow the universal T_c vs δ relation. Magnetic measurements reveal that increasing δ enlarges the field and temperature stability of the Bragg glass phase. These findings imply that the interlayer coupling between Cu-O layers enhances with δ . The anisotropy parameter estimated from directional first-penetration field measurements monotonously decreases from 50 in the underdoped (UD) to 15 in the OD regimes. However, the in-plane penetration depth presents a boomerang-type behavior with δ , reaching its minimum value close to optimal doping. These two facts lead to a crossover from a Josephson OD to electromagnetic UD-dominated coupling of adjacent Cu-O layers in the vicinity of optimal doping.

DOI: [10.1103/PhysRevB.77.184508](https://doi.org/10.1103/PhysRevB.77.184508)

PACS number(s): 74.72.Hs, 74.62.Dh, 74.25.Dw, 74.25.Ha

I. INTRODUCTION

Understanding the extremely anisotropic electronic and magnetic properties of layered cuprates requires unveiling the nature of the coupling mechanism between the superconducting Cu-O layers. In these materials, these layers are composed of a stack of Cu-O planes. The interlayer coupling between adjacent Cu-O layers is produced by Josephson tunneling and by electromagnetic interactions between the supercurrents lying in the layers.^{1,2} The family of Bi-based compounds presents a weak interlayer coupling between the Cu-O layers³ resulting in both terms being comparable. The possibility of the electromagnetic interaction being dominant over the Josephson one was thoroughly studied³⁻⁵ for the bilayer $\text{Bi}_2\text{Sr}_2\text{CaCu}_2\text{O}_{8+\delta}$ (Bi-2212) compound, which presents one of the weakest interlayer coupling among cuprates.³ In this work, we address this issue in the less studied three-layer $\text{Bi}_2\text{Sr}_2\text{Ca}_2\text{Cu}_3\text{O}_{10+\delta}$ (Bi-2223) material by tuning the oxygen concentration in a single sample. Such studies in this compound are lacking because of the difficulty in obtaining pure- and high-quality macroscopic crystals⁶ for reliable magnetic measurements. This compound presents the highest critical temperature at optimal doping (OPT) among Bi-based cuprates, $T_c^{\text{OPT}} = 110.5$ K. To the best of our knowledge, the study presented here constitutes the first exhaustive survey on the effect of oxygen-doping on the vortex phase diagram of a three-layer cuprate compound.

The crystal structure of Bi-2223 is composed of insulating (Bi-O-Sr-O blocking) layers intercalating in the c -axis direction with superconducting Cu-O layers. The spacing between the layers, each one formed by three Cu-O planes, is $s = 18$ Å for optimally doped samples.⁷ The interlayer coupling is inversely proportional to the electronic anisotropy $\gamma = \sqrt{m_c/m_{ab}}$, which is given by the ratio between the effective masses in the c axis and in the ab plane.¹ As mentioned, this coupling is produced by two different mechanisms. The first, the Josephson coupling, consists of the hole tunneling

from one Cu-O layer to the adjacent through the blocking layer. This mechanism is dominant when $s\gamma < \lambda_{ab}(0)^2$, where $\lambda_{ab}(0)$ is the in-plane penetration depth. The second mechanism arises from the electromagnetic interaction between the supercurrents located in adjacent Cu-O layers and is, on the contrary, dominant when $s\gamma > \lambda_{ab}(0)^2$. The relevance of these two mechanisms depends on the hole-carrier concentration and on the degree of charge transfer between the Cu-O layers. One way to modify these magnitudes is to overdope (OD) or underdope (UD) with respect to the optimal oxygen content ($\delta = \delta_{\text{OPT}}$). Extra oxygen atoms will occupy vacancies in the blocking layers.

Oxygen-doping produces quantitative changes in the vortex phase diagram. The flux lines in extremely anisotropic Bi-based cuprates are composed of a stack of poorly coupled pancake vortices located in the Cu-O layers.¹ This weak coupling leads to the liquid vortex phase, spanning a considerable fraction of the H - T phase diagram.⁸ Upon cooling at low magnetic fields, vortex matter undergoes a first-order solidification transition at T_m .^{8,9} Upon further cooling, the vortex magnetic response becomes irreversible since pinning sets in at a temperature $T_{\text{IL}}(H) \approx T_m(H)$, the so-called irreversibility line. The stable phase at low temperatures, which is the Bragg glass,^{10,11} exhibits quasicrystalline order. With increasing magnetic field, the vortex structure transforms into a topologically disordered glass¹² through a first-order phase transition known as the second-peak line H_{SP} .^{13,14} The vortex glass melts with increasing temperature through a second-order phase transition.¹⁵ In the case of Bi-2212, the Bragg glass phase spans up to higher temperatures and fields with increasing oxygen concentration,^{5,14,16} which is consistent with a decrease in γ with δ . Introducing extra oxygen atoms also affects the pinning potential landscape.¹⁷ Nevertheless, changes in the vortex phase diagram provide information on the evolution of the interlayer coupling with doping. In this work, we report on the doping dependence of the critical current density $J_c(T, H)$ and on the evolution of

$H_{SP}(T)$, $H_{IL}(T)$, and $T_{0D}(H)$, the zero-dimensional pinning temperature at which pancake vortices of every Cu-O layer are individually pinned. We find that changes in the oxygen-doping level of Bi-2223 affect the vortex phase diagram in a similar manner to that of Bi-2212. However, since Bi-2223 is three times less anisotropic than Bi-2212, significant differences are also detected.

In the case of the bilayer compound, increasing the oxygen concentration results in a monotonous reduction in γ (Refs. 3 and 5) and of the c -axis lattice parameter,⁵ and consequently s . However, $\lambda_{ab}(0)$ evolves in a nonmonotonous way with δ being minimum in the slightly OD regime.^{4,5,18,19} Therefore, given that in Bi-based compounds $s\gamma \sim \lambda_{ab}$, a crossover from electromagnetic to Josephson-dominated coupling is quite likely when decreasing δ . Evidence of this crossover was indeed reported in the case of Bi-2212.⁵ Nevertheless, as the anisotropy of Bi-2223 is smaller than that of Bi-2212; in the three-layer compound, the Josephson coupling might be dominant in a wider δ region. In this work, we address the question of whether a crossover from Josephson to electromagnetic coupling is plausible in Bi-2223. We find that when decreasing δ , on top of increasing the magnitude of the electronic anisotropy, this crossover takes place in the vicinity of optimal doping.

II. CRYSTAL GROWTH AND OXYGEN-DOPING

Bi-2223 and Bi-2212 crystals were grown by means of the traveling-solvent floating-zone method as described in Ref. 6. The structural and superconducting properties of the crystals used in this work are reported in Refs. 7 and 20. X-ray diffraction measurements have revealed the phase purity and the high crystalline order of our samples. In the case of the Bi-2223 samples, its quality has allowed the refinement of the crystal structure from single-crystal x-ray diffraction data.⁷ Electrical resistivity and magnetic measurements reveal a single and sharp superconducting transition. For example, Fig. 1(b) shows the low field susceptibility of the sample studied for the UD, OPT, and OD regimes and Fig. 1(c) shows the field-cooling magnetization vs temperature curves for low and high applied fields in the case of the OPT regime. By considering the measurements resolution, these results indicate that if present, Bi-2212 intergrowths represent less than 1% of the volume of the samples.

In order to tune and to homogenize the hole concentration, the crystals were annealed for 10 days at 500 °C under various oxygen partial pressures $p(O_2)$. In Fig. 1, we compare the dependences of T_c on $p(O_2)$ for both the Bi-2212 and the Bi-2223 crystals. Every point results from an average over at least ten samples annealed in the same conditions. At every $p(O_2)$ value, the critical temperature and the transition width are the same within the error, as measured by means of ac susceptibility and dc magnetization. The reliability of these results allows us to consider the critical temperature as a measure of the macroscopic oxygen content. The transition temperature T_c is taken as the temperature at which $\partial\chi'/\partial T$ and $\partial M/\partial T$ exhibit a peak. The transition widths are estimated as the FWHM of these peaks and range from 0.6 to 2 K. This is an indication that in our crystals, the oxygen distribution is rather homogeneous.

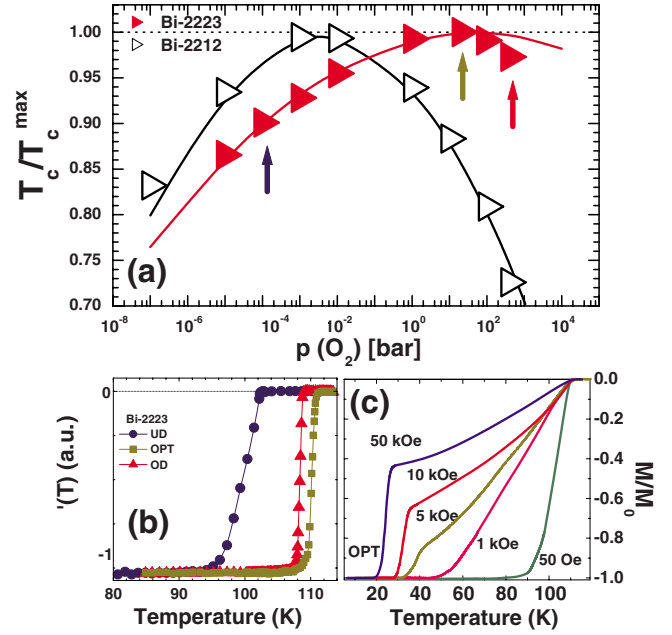


FIG. 1. (Color online) (a) Normalized critical temperature as a function of postannealing oxygen pressure $p(O_2)$ for Bi-2223 and Bi-2212. The maximum values of the critical temperature are (90.5 ± 0.5) and (110.5 ± 0.5) K for Bi-2212 and Bi-2223, respectively. The lines are fits of the data with the universal relation $T_c = T_c^{\max} [1 - 82.6(\delta - 0.27)^2]$ (Refs. 21–23) with $\delta = 0.011 \ln p(O_2) + 0.3$ (Ref. 23) for Bi-2212 and $\delta = 0.006 \ln p(O_2) + 0.26$ for Bi-2223. Every point in $p(O_2)$ corresponds to at least ten samples and the size of the points indicates the dispersion in critical temperature. The arrows indicate the different doping levels tuned in the sample used to study the doping dependence of the Bi-2223 vortex phase diagram. (b) Real part of the susceptibility as a function of temperature for the same sample of Bi-2223 in the UD [$T_c(100 \pm 2)$ K], OPT [$T_c(110.5 \pm 0.5)$ K], and OD [$T_c(107 \pm 0.5)$ K] regimes. The $\chi'(T)$ measurements were performed with an ac field of 0.1 Oe in magnitude and 970 Hz in frequency. (c) Temperature evolution of the field-cooled magnetization normalized by the low-temperature saturation value (M_0) for the OPT regime. The applied magnetic fields range between 50 Oe and 50 kOe.

In the case of the Bi-2212 samples, the T_c vs $p(O_2)$ data are in quantitative agreement with existing literature³ and do not deserve any further comment. However, the results for Bi-2223 are in qualitative disagreement with previous reports.^{24,25} As in the case of these works, our OPT Bi-2223 samples, with $T_c = (110.5 \pm 0.5)$ K, are obtained at a quite high partial pressure $p(O_2^{\text{OPT}}) = 20$ bar. For higher annealing pressures, the samples become overdoped. Figure 1 shows that T_c does change in the OD regime, decreasing from (110.5 ± 0.5) to (107.0 ± 0.5) K. This is in contrast to the works of Fujii *et al.*²⁴ and Liang *et al.*,²⁵ which reported a T_c vs $p(O_2)$ plateau in the OD regime. The authors^{24,25} claimed that this plateau results from a different doping level of the inner and outer planes of the Cu-O layers, the inner being less doped.²⁶ This interpretation is based on a theoretical model that assumes a strong interlayer coupling.²⁷

In spite of the inner and outer Cu-O planes having a different doping level,²⁶ other factors might be at the origin of the T_c plateau reported in Refs. 24 and 25. As a matter of

fact, an inhomogeneous oxygen distribution throughout the sample can be responsible for an apparent insensitivity of T_c to oxygen-doping. An inhomogeneous oxygen distribution is also compatible with the detected decrease in the c -axis lattice parameter²⁴ and the enhancement of the vortex irreversibility field²⁵ with increasing δ . Crystals exhibiting a superconducting transition broader than ours, such as the ones reported in Refs. 24 and 25, might present an inhomogeneous oxygen spatial distribution. In such crystals, the onset of the superconducting transition would be determined by the OPT domains, whereas the shift in the x-ray reflections and the enhancement of $H_{IL}(T)$ would be dominated by the OD ones. The narrower superconducting transitions measured in our crystals indicate that their spatial oxygen distribution is more homogeneous and as a consequence, the detected decrease in T_c in the OD regime is not hidden by inhomogeneities of the samples.

The most striking result of Fig. 1 is that a larger oxygen partial pressure is required in order to reach optimal doping in Bi-2223 than in Bi-2212. Our results for the Bi-2212 samples are in agreement with the established bell-shaped dependence of T_c on oxygen concentration;^{21–23} see fits of Fig. 1. On the contrary, in the case of Bi-2223, the curve resulting from adjusting the UD data with the universal T_c vs doping [$p(O_2)$] relation^{21,22} does not fit the points in the OD regime. Seminal works on three-layer cuprates already reported that T_c follows the universal law in the UD region.^{22,28} Our results in Bi-2223 confirm this and also indicate that in the OD regime of three-layer compounds, the universal law^{21,22} is not fulfilled, as in the case of single- and bilayer cuprates. This phenomenology can be related to the different doping level of the outer and inner Cu-O planes.

III. DOPING DEPENDENCE OF THE VORTEX PHASE DIAGRAM

As mentioned, to study the effect of hole-doping on the vortex phase diagram of Bi-2223, the oxygen content was tuned in the same sample. The results presented in this section correspond to doping levels in the UD [$T_c = (100 \pm 2)$ K], OPT [$T_c = (110.5 \pm 0.5)$ K], and OD [$T_c = (107.0 \pm 0.5)$ K] regimes.

The vortex phase diagram was studied by means of bulk magnetic measurements using a Quantum-design superconducting quantum interference device (SQUID) magnetometer and a physical properties measurement systems (PPMS) measurement system. In particular, we report on the evolution of the irreversibility line $H_{IL}(T)$, the order-disorder $H_{SP}(T)$ transition line, which is associated with a peak in the critical current,^{13,14} and the zero-dimensional pinning line T_{OD} .^{29,30} These lines were obtained from the magnetization vs temperature measurements $M(T)$, following the zero-field-cooling (ZFC) and field-cooling (FC) paths, and from the hysteresis magnetization loops $M(H)$. For these measurements, the field was applied out of plane, i.e., $H \parallel c$ axis. The typical field and temperature sweep rates in $M(H)$ and $M(T)$ measurements were 10^{-2} G/s and 10^{-3} K/s, respectively. Figure 2 presents typical magnetization data for doping levels corresponding to the UD, OPT, and OD regimes. The supercon-

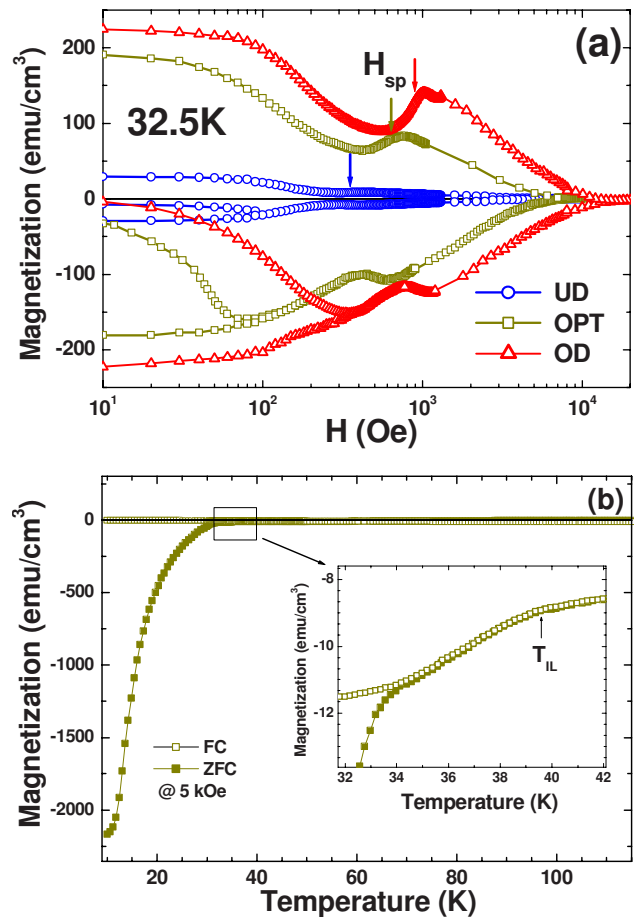


FIG. 2. (Color online) (a) Magnetization loops at 32.5 K for the same sample for UD [$T_c = (100 \pm 2)$ K], OPT [$T_c = (110.5 \pm 0.5)$ K], and OD [$T_c = (107.0 \pm 0.5)$ K] oxygen concentrations. The second peak field $H_{SP}(T)$ is indicated by arrows. (b) Field-cooling (FC) and zero-field-cooling (ZFC) magnetization measurements for the OPT regime at an applied field of 5 kOe. The onset temperature of the irreversible magnetic behavior at 5 kOe, T_{IL} , is indicated.

ducting transition in each case is shown in the inset of Fig. 1.

The onset of the irreversible magnetic response was obtained from the field- and zero-field-cooling $M(T)$ curves when the kink was detected at a temperature higher than $T_{IL}(H)$ where both branches merge;³¹ see Fig. 2(b). The hole-doping dependence of the irreversibility line is shown in the H vs. T/T_c phase diagram of Fig. 3. At any reduced temperature, the irreversibility field is enhanced by increasing the oxygen-doping level. The evolution of $H_{IL}(T)$ with doping for the bilayer compound⁵ and data previously reported for Bi-2223^{25,32} follow the same trend.

The enlargement of the solid vortex phase is consistent with an enhancement of the interlayer coupling by increasing oxygen concentration and consequently a reduction in the anisotropy parameter. Theoretical studies indicated that the melting³³ and decoupling³⁴ lines shift toward higher temperatures as soon as a small Josephson coupling between the layers is considered on top of the electromagnetic interactions. In the case of plateletlike samples, such as the ones studied in this work, for Bi-2212 at low fields, the irrevers-

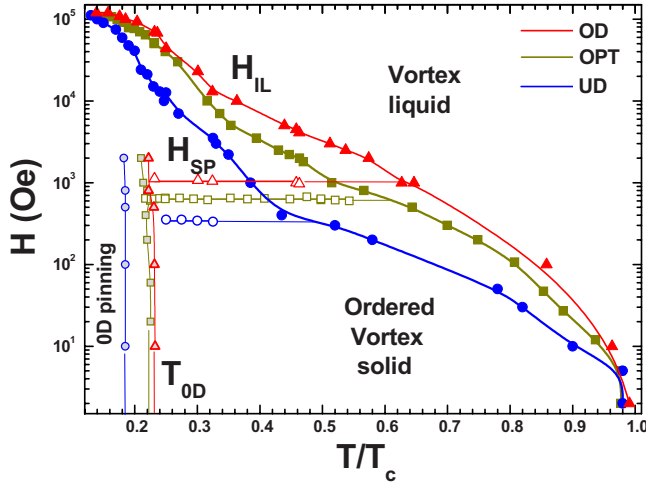


FIG. 3. (Color online) Vortex phase diagram for the same sample in UD (\circ), OPT (\square), and extremely OD (\triangle) regimes. The irreversibility, $H_{IL}(T)$ (full symbols), second peak $H_{SP}(T)$ (open symbols), and zero-dimensional pinning $T_{0D}(H)$ (gray filled symbols) lines are shown. The error in magnetic field and temperature of the measured points is included in their size.

ibility coincides with the melting and decoupling lines.^{8,30} Therefore, the enhanced stability of the solid vortex phase shown in Fig. 3 can be associated with an increasingly relevant role of the Josephson coupling when raising the doping level. This is quite likely since $s\gamma \gtrsim \lambda_{ab}$ for the OPT regime of Bi-2223. This issue will be further discussed in the next section.

The transition line $H_{SP}(T)$ is manifested as a peak-valley structure in the $M(H)$ curves, as evident in the magnetization loops of Fig. 2(a). We considered $H_{SP}(T)$ to be the field at which M has an inflection point between the peak and the valley (indicated by arrows in the figure), averaging the values for the two branches of the loop. The phase diagram of Fig. 3 shows that the second-peak line is roughly temperature-independent, as also found in Bi-2212.^{5,14,30} Theoretical works considering the $H_{SP}(T)$ line as an order-disorder phase transition between the low-field Bragg glass and the high-field vortex glass^{11,35} estimate $H_{SP}(T)$ as the field where the elastic energy of the vortex structure equals the pinning energy. These two energy terms depend on the penetration depth, coherence length, and anisotropy of the material, as well as on the pinning parameter.¹¹ Therefore, the temperature evolution of H_{SP} is determined by the temperature dependence of λ_{ab} and ξ_{ab} .³⁶ Figure 3 shows that for the three doping levels studied, H_{SP} is detected only in the temperature range $0.2 \lesssim T/T_c \lesssim 0.55$. By considering the two-fluid expression for λ_{ab} and ξ_{ab} ,¹ in this temperature range, both magnitudes vary within 3%. This minimal variation and the important anisotropy³⁶ of the material are responsible for the observed roughly temperature-independent H_{SP} .

The temperature-averaged H_{SP} increases with doping: (340 ± 20) Oe for the UD, (630 ± 40) Oe for the OPT, and (1040 ± 60) Oe for the OD regimes. The same qualitative behavior was reported in Bi-2212^{5,14,16} and other cuprates.³⁷ The evolution of $H_{SP}(T)$ with doping is consistent with an

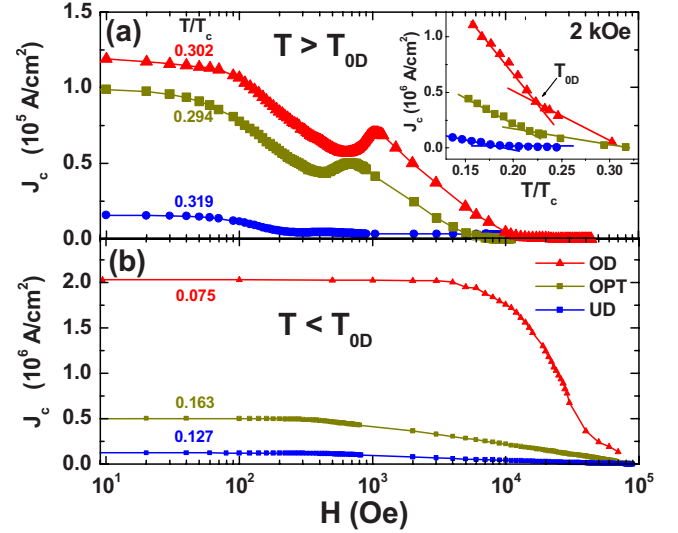


FIG. 4. (Color online) Critical current density as a function of magnetic field $J_c(H)$ for (a) $T > T_{0D}$ and (b) $T < T_{0D}$. Inset: Curves of J_c vs reduced temperature obtained from the width of the magnetization loop at 40 Oe (see text). The arrows indicate the kink in J_c considered as the temperature T_{0D} at which the zero-dimensional pinning sets in.

enhancement of coupling between the Cu-O planes with increasing oxygen concentration, as also suggested by the doping dependence of $H_{IL}(T)$.² This point will be further discussed in Sec. IV.

The zero-dimensional pinning line T_{0D} that separates the regime where individual pancake vortices are pinned ($T < T_{0D}$) from that where vortex lines are individually pinned can be obtained from critical current density vs temperature curves $J_c(T)$ at a given magnetic field.³⁸ In the low-temperature zero-dimensional pinning regime, not only the vortex-pinning interaction overcomes the vortex-vortex interaction but also pancake vortices belonging to the same vortex but to different Cu-O layers are individually pinned.¹ Therefore, at temperatures $T < T_{0D}$, the critical current should be field independent at low fields. This is a consequence of the c -axis Larkin correlation length, $L_c^c \sim (r_p/\gamma)(J_0/J_c)^{1/2}$,³⁹ becoming smaller than the Cu-O layers spacing s .¹ In the last expression, $r_p \sim \xi$ is the typical pinning range and $J_0 = 4c\Phi_0/12\sqrt{3}\pi\lambda_{ab}^2\xi_{ab}$ is the depairing current density. Therefore, $T_{0D}(T)$ can be estimated as the temperature at which $J_c(T)$ presents a kink and a steeper increase in the low-temperature region.³⁸ In this work, we consider the same criterion to estimate T_{0D} .

The critical current is obtained from the magnetization loops measured at different temperatures, as shown in Fig. 2(a). By considering the Bean model,⁴⁰ at a given temperature, $J_c(T, H) \sim (3c/2R)\Delta M(T, H)$, where $\Delta M(T, H)$ is the separation between the two branches of the magnetization loop at a field H , c is the speed of light, and R is the radius of an equivalent cylindrical sample.⁴⁰ Figure 4 reveals that the critical current of Bi-2223 is 1 order of magnitude larger than that of Bi-2212³⁸ at similar reduced temperatures and fields. From Fig. 4, it is also evident that at low temperatures, the critical current is field independent at low fields, which is

a fingerprint of the individual pinning regime (either of flux lines or of individual pancakes). The inset of Fig. 4 shows typical $J_c(T/T_c)$ curves at an applied field of 40 Oe for the UD, OPT, and OD regimes. The kink in critical current identified as T_{0D} is indicated by arrows. By considering that for the OPT regime of Bi-2223 $\xi \sim 10 \text{ \AA}$,⁴¹ $J_0 = 6.15 \cdot 10^8 \text{ \AA/cm}^2$, $\gamma = 27 \pm 4$ (see the data shown in Sec. IV), and $J_c(T_{0D}) = 1.81 \times 10^5 \text{ \AA/cm}^2$, a value of $L_c^c = 24\text{--}18$ close to s is estimated at $T = T_{0D}$. Similar values for L_c^c are obtained for the UD and OD regimes.

For every doping level, the zero-dimensional-pinning line is roughly field independent, as also found in Bi-2212.^{5,30} Since T_{0D} is the temperature at which the individual pinning of pancake vortices sets in, then $J_c(T)$ is almost field independent for $T \leq T_{0D}$. Therefore, $L_c^c \sim (r_p/\gamma)[J_0/J_c(T_{0D})]^{1/2}$ equals the Cu-O layers spacing at a temperature T_{0D} that is roughly field independent. The location of T_{0D} is however doping dependent. The zero-dimensional pinning line is placed at (18.5 ± 0.5) K for the UD, (24 ± 1) K for the OPT, and (25 ± 1) K for the OD regimes. A study on the OPT and OD regime of Bi-2212 samples reports that T_{0D} does not significantly change with doping.³⁸ However, as the magnitude of $J_c(T_{0D})$ is in direct relation with T_{0D} (see Fig. 4), if γ decreases, then, in order to fulfill $L_c^c = s$, $J_c(T_{0D})$ and therefore T_{0D} have to increase. The difference between our results for Bi-2223 and those reported for Bi-2212³⁸ might originate from the fact that in the latter study, the anisotropy changes are on the order of 30% whereas in our case, they are 5 times greater than this value (see Sec. IV for the detailed data in this respect). Therefore, an increment of the zero-dimensional temperature with doping is in agreement with the enhancement of interlayer coupling, which is suggested by the doping evolution of $H_{IL}(T)$ and $H_{SP}(T)$.

One interesting result of the vortex phase diagrams shown in Fig. 3 is that for $T < T_{0D}$, the order-disorder second peak line is no longer detected within our experimental resolution. Similar findings were observed in Bi-2212 samples.^{30,38} The vortex glass phase located at $H > H_{SP}$ presents no vortex phase correlation in the c direction,³⁰ whereas the zero-dimensional pinning region is correlated in the ab plane as well as in the perpendicular direction.³⁸ Therefore, the suppression of the vortex phase correlation along the c direction takes place only when L_c^c exceeds the spacing between the Cu-O layers. This suggests that the establishment of a zero-dimensional pinning regime inhibits the vortex structure instability associated with the order-disorder phase transition detected at $T > T_{0D}$.

In summary, the doping dependence of the transition lines $H_{IL}(T)$ and $H_{SP}(T)$ and the crossover temperature T_{0D} are in agreement with an enhancement of the coupling between Cu-O layers with increasing doping. The decrease in γ on overdoping, which is suggested by the results presented in this section, implies that the Josephson coupling term between adjacent layers becomes increasingly relevant. Therefore, the scenario of a crossover from an electromagnetic UD to a Josephson OD-dominated interlayer coupling is quite likely. However, a possible nonmonotonous evolution of λ_{ab} with doping has to be explored in order to differentiate between this scenario and the situation where the interlayer coupling increases but continues to be electromagnetic in nature when overdoping.

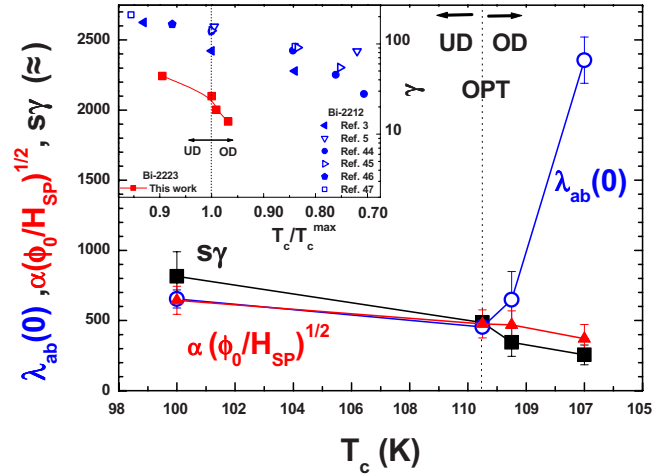


FIG. 5. (Color online) Evolution of the in-plane penetration depth $\lambda_{ab}(0)$, the anisotropy $s\gamma$, and the second-peak field $\alpha \sqrt{\Phi_0/H_{SP}}$, for the UD, OPT, and OD regimes of Bi-2223. Inset: Electronic anisotropy as a function of T_c/T_c^{\max} for our Bi-2223 sample and values reported in literature for numerous Bi-2212 samples (Refs. 3, 5, and 43–47).

IV. CROSSOVER FROM ELECTROMAGNETIC TO JOSEPHSON COUPLING WHEN OVERDOPING

In order to study the nature of the coupling between the Cu-O layers of Bi-2223 as a function of doping, we quantitatively compared the characteristic lengths $s\gamma$ and λ_{ab} . In the case of Bi-2212, a crossover from electromagnetic ($s\gamma > \lambda_{ab}$) to Josephson ($s\gamma < \lambda_{ab}$)-dominated interlayer coupling takes place slightly above the OPT regime (for $T_c \sim 0.9T_c^{\max}$).⁵ We study this possibility in the case of Bi-2223.

The in-plane penetration depth is extracted from the measurements of the first penetration field with H applied perpendicular to the Cu-O planes, H_{c1}^\perp , for different temperatures in the range 35–60 K. The first penetration field was obtained from the M vs H loops, where the magnetic relaxation at every field was measured for 1 h. This was done in order to avoid the effect of surface and geometrical pinning barriers.⁴² The effective first-penetration field for the sample was considered as that where the magnetization shows a detectable relaxation, which is associated with the entrance of the first vortex. The effect of the demagnetizing factor of the sample estimated from the Meissner slope was considered in order to obtain H_{c1}^\perp . The value of $\lambda_{ab}(0)$ was obtained by fitting the temperature-dependent H_{c1}^\perp within the London model, $H_{c1}^\perp = \Phi_0/[4\pi\lambda_{ab}(T)^2] \ln[\lambda_{ab}(T)/\xi_{ab}(T)]$, and considering the two-fluid model expressions for $\lambda_{ab}(T)$ and $\xi_{ab}(T)$.¹ The zero-temperature coherence length is taken as $\xi(0) = 10 \text{ \AA}$, as suggested by scanning tunneling microscopy (STM) measurements of the superconducting density of states in the vicinity of a vortex.⁴¹

The boomeranglike dependence of $\lambda_{ab}(0)$ on oxygen concentration is shown in Fig. 5: it decreases from the UD toward the OPT region and then substantially increases in the OD regime. This nonmonotonous evolution is in agreement with the results obtained in other cuprates.^{4,19,48} It was originally proposed that this decrease in the superfluid density in

the OD regime results from a substantial pair breaking in spite of the normal-state carrier concentration, increasing when overdoping.¹⁹ However, (SMT) data on several cuprates are at odds with this interpretation since the superconducting quasiparticle peaks sharpen on increasing doping.⁴⁹ Therefore, the origin of this phenomenon remains still as an open question.

The anisotropy parameter is estimated from the first penetration field for H , which is applied perpendicular and parallel to the Cu-O planes since within the London approximation, $\gamma = H_{c1}^{\perp}/H_{c1}^{\parallel}$.¹ The values of H_{c1}^{\parallel} were measured by aligning the sample with a homemade rotation system that reduces the misalignment uncertainty to $\sim 0.5^{\circ}$. The effect of the demagnetizing factor was corrected from the Meissner slope, giving a value in accordance to the $D_{\parallel} \sim (1 - D_{\perp})/2$ relation found for plateletlike samples. The values of γ presented in the inset of Fig. 5 correspond to the averaged results obtained at different temperatures, ranging between 35 and 60 K. The error bar in the points represents the dispersion of values measured at different temperatures. The anisotropy parameter monotonically decreases with increasing oxygen concentration. This establishes that the interlayer coupling is enhanced by increasing the oxygen concentration, as suggested by the results presented in Sec. III. We estimate a value of $\gamma = (27 \pm 3)$ for the optimally doped sample, smaller than previously reported.⁵⁰ It is important to point out that our estimation is a result of measuring the first critical field at various temperatures whereas in Ref. 50, it was estimated from the measurements at a single temperature.

The same evolution of the anisotropy parameter with oxygen-doping was found for Bi-2212, one of the most anisotropic cuprates. The inset of Fig. 5 compares the evolution of γ to T_c/T_c^{\max} for the bilayer and three-layer Bi-based compounds. Although the Bi-2212 data are roughly three times larger than the Bi-2223 ones, the variation in γ relative to γ^{OPT} is similar in both compounds. Therefore, the coupling between the Cu-O layers of Bi-2223 is affected by oxygen-doping in a similar amount, relative to γ^{OPT} , than in Bi-2212.

Changes in the oxygen concentration affect the anisotropy parameter mostly because the number of carriers in the charge reservoir blocks varies but also because the c -axis lattice parameter is slightly modified. Adding extra oxygen reduces the c -axis lattice parameter and therefore s .⁵ In the case of Bi-2212, the overdoping-induced decrease in the c -axis lattice parameter was found to be of only $\sim 0.5\%$.⁵ This change is much smaller than the error we have in determining γ and therefore in estimating $s\gamma$, we consider the value $s = 18$ Å, which is measured in OPT samples as the spacing between the Cu-O layers at all doping levels.

Another parameter that gives information on the nature of the interlayer coupling is the doping evolution of $\sqrt{\Phi_0/H_{\text{SP}}}$. In the case of the interlayer coupling being dominated by the electromagnetic term, $\sqrt{\Phi_0/H_{\text{SP}}} \propto \lambda_{ab}$.² On the contrary, if the Josephson interaction dominates, $\sqrt{\Phi_0/H_{\text{SP}}} \propto s\gamma$.² Figure 5 shows that $\sqrt{\Phi_0/H_{\text{SP}}}$ monotonously decreases with doping and therefore significantly deviates from the evolution of λ_{ab} with doping in the OD regime.

To summarize, Fig. 5 shows a comparison of the characteristic lengthscales. In the OD regime, $s\gamma < \lambda_{ab}(0)$ and

$\sqrt{\Phi_0/H_{\text{SP}}}$ does not follow the trend of $\lambda_{ab}(0)$ but rather that of $s\gamma$. These findings indicate that the Josephson interaction progressively dominates the interlayer coupling with increasing oxygen concentration from optimal doping. At the OPT regime, $s\gamma$ becomes of the order of the in-plane penetration depth. Deep into the UD region, $s\gamma$ slightly overcomes $\lambda_{ab}(0)$ and $\sqrt{\Phi_0/H_{\text{SP}}}$ follows the same trend with that of the penetration depth. These results constitute evidence that in the UD regime, the interlayer coupling is dominated by the electromagnetic term. Therefore, with increasing doping from the UD to the OD regime, not only the anisotropy decreases but the coupling between Cu-O layers changes in nature, presenting a crossover from an electromagnetic to a Josephson-dominated interaction. Although with our data, the exact doping level at which this crossover takes place cannot be accurately determined, it is evident that it occurs in the vicinity of the OPT regime.

V. CONCLUSIONS

We provide evidence that oxygen-doping in Bi-2223 crystals produces a non-negligible change in T_c in the OD regime, in contrast to previous claims.^{24,25} The changes in T_c/T_c^{\max} are nonsymmetrical with respect to optimal doping: in the OD regime, they are greater than in the UD regime. Therefore, the evolution of T_c in the OD regime of Bi-2223 does not follow the universal relation with δ as found in many single- and bilayer cuprates.^{21,22}

Varying oxygen concentration affects the vortex matter phase diagram in a way that is consistent with an enhancement of the Cu-O interlayer coupling with increasing δ . Namely, the Bragg glass phase spans up to higher fields [$H_{\text{SP}}(T)$ increases] and temperatures [$T_{\text{IL}}(H)$ and $T_{\text{OD}}(H)$ increase] when overdoping. The evolution of $H_{\text{IL}}(T)$ and $H_{\text{SP}}(T)$ with doping is in agreement with results reported for the bilayer parental compound.^{3,5,14} In the case of the zero-dimensional pinning temperature, we do detect an increase in δ contrary to reports on Bi-2212.³⁸ This can be understood, considering that in our work, δ is varied in a much larger interval than in Ref. 38.

The suggested enhancement of the interlayer coupling with increasing δ is indisputably observed by the monotonous decrease in anisotropy with oxygen concentration. A comparison between the directly measured magnitudes $s\gamma$, λ_{ab} , and $\sqrt{\Phi_0/H_{\text{SP}}}$ reveals that a crossover from Josephson OD to electromagnetic UD-dominated coupling takes place around optimal doping. This crossover originates from the nonmonotonous behavior of λ_{ab} with δ . Therefore, the highly anisotropic superconducting properties of UD Bi-2223 rely not only on a decrease in the magnitude of the Cu-O layer interaction but also in a change in the nature of its coupling mechanism.

ACKNOWLEDGMENTS

The authors acknowledge G. Nieva for useful discussions and R. Lortz for assistance in the SQUID measurements. This work was supported by the MANEP National Center of Competence in Research of the Swiss National Science Foundation.

- *alexandre.piriou@physics.unige.ch
- ¹G. Blatter, M. V. Feigelman, V. B. Geshkenbein, A. I. Larkin, and V. M. Vinokur, *Rev. Mod. Phys.* **66**, 1125 (1994).
 - ²A. E. Koshelev and V. M. Vinokur, *Phys. Rev. B* **57**, 8026 (1998).
 - ³K. Kishio, in *Coherence in High Temperature Superconductors*, edited by G. Deutscher and A. Revcolevschi (World Scientific, Singapore, 1996), p. 212, and references therein.
 - ⁴G. Villard, D. Pelloquin, and A. Maignan, *Phys. Rev. B* **58**, 15231 (1998).
 - ⁵V. F. Correa, E. E. Kaul, and G. Nieva, *Phys. Rev. B* **63**, 172505 (2001).
 - ⁶E. Giannini, V. Garnier, R. Gladyshevskii, and R. Flükiger, *Supercond. Sci. Technol.* **17**, 220 (2004).
 - ⁷E. Giannini, R. Gladyshevskii, N. Clayton, N. Musolino, V. Garnier, A. Piriou, and R. Flükiger, *Curr. Appl. Phys.* **8**, 115 (2008).
 - ⁸H. Pastoriza, M. F. Goffman, A. Arribére, and F. de la Cruz, *Phys. Rev. Lett.* **72**, 2951 (1994).
 - ⁹E. Zeldov, D. Majer, M. Konczykowski, V. B. Geshkenbein, V. M. Vinokur, and H. Shtrikman, *Nature (London)* **375**, 373 (1995).
 - ¹⁰T. Nattermann, *Phys. Rev. Lett.* **64**, 2454 (1990).
 - ¹¹T. Giamarchi and P. Le Doussal, *Phys. Rev. Lett.* **72**, 1530 (1994).
 - ¹²D. S. Fisher, M. P. A. Fisher, and D. A. Huse, *Phys. Rev. B* **43**, 130 (1991).
 - ¹³R. Cubbitt, E. M. Forgan, G. Yang, S. L. Lee, D. McK. Paul, H. A. Mook, M. Yethiraj, P. H. Kes, T. W. Li, A. A. Menovsky, Z. Tarnawski, and K. Mortensen, *Nature (London)* **365**, 407 (1993); E. Zeldov, D. Majer, M. Konczykowski, A. I. Larkin, V. M. Vinokur, V. B. Geshkenbein, N. Chikumoto, and H. Shtrikman, *Europhys. Lett.* **30**, 367 (1995).
 - ¹⁴B. Khaykovich, E. Zeldov, D. Majer, T. W. Li, P. H. Kes, and M. Konczykowski, *Phys. Rev. Lett.* **76**, 2555 (1996).
 - ¹⁵B. Khaykovich, M. Konczykowski, E. Zeldov, R. A. Doyle, D. Majer, P. H. Kes, and T. W. Li, *Phys. Rev. B* **56**, R517 (1997).
 - ¹⁶K. Kishio, J. Shimoyama, Y. Kotaka, and K. Yamafuji, in *Proceedings of the Seventh International Workshop on Critical Currents in Superconductors*, edited by H. W. Weber (World Scientific, Singapore, 1994), p. 339; C. Bernhard, C. Wenger, Ch. Niedermayer, D. M. Pooke, J. L. Tallon, Y. Kotaka, J. Shimoyama, K. Kishio, D. R. Noakes, C. E. Stronach, T. Sembiring and E. J. Ansaldo, *Phys. Rev. B* **52**, R7050 (1995); C. M. Aegerter, S. L. Lee, H. Keller, E. M. Forgan, and S. H. Lloyd, *ibid.* **54**, R15661 (1996); T. Tamegai, M. Tokunaga, S. Kasahara, M. Matsui, and H. Akoi, in *Proceedings of the Ninth International Symposium on Superconductivity*, edited by S. Nakajima and M. Murakami (Springer-Verlag, Tokyo, 1997), p. 621.
 - ¹⁷S. Ooi, T. Shibauchi, and T. Tamegai, *Physica C* **302**, 339 (1998).
 - ¹⁸Y. J. Uemura, G. M. Luke, B. J. Sternlieb, J. H. Brewer, J. F. Carolan, W. N. Hardy, R. Kadono, J. R. Kempton, R. F. Kiefl, S. R. Kretzman, P. Mulhern, T. M. Riseman, D. L. Williams, B. X. Yang, S. Uchida, H. Takagi, J. Gopalakrishnan, A. W. Sleight, M. A. Subramanian, C. L. Chien, M. Z. Cieplak, Gang Xiao, V. Y. Lee, B. W. Statt, C. E. Stronach, W. J. Kossler, and X. H. Yu, *Phys. Rev. Lett.* **62**, 2317 (1989); Y. J. Uemura, L. P. Le, G. M. Luke, B. J. Sternlieb, W. D. Wu, J. H. Brewer, T. M. Riseman, C. L. Seaman, M. B. Maple, M. Ishikawa, D. G. Hinks, J. D. Jorgensen, G. Saito, and H. Yamochi, *ibid.* **66**, 2665 (1991).
 - ¹⁹Ch. Niedermayer, C. Bernhard, U. Binniger, H. Glückler, J. L. Tallon, E. J. Ansaldo, and J. I. Budnick, *Phys. Rev. Lett.* **71**, 1764 (1993).
 - ²⁰E. Giannini, N. Clayton, N. Musolino, R. Gladyshevskii, and R. Flükiger, in *Frontiers in Superconducting Materials*, edited by A. Narlikar (Springer-Verlag, London, 2005), p. 739.
 - ²¹C. Allgeier and J. S. Schilling, *Physica C* **168**, 499 (1990).
 - ²²M. R. Presland, J. L. Tallon, R. G. Buckley, R. S. Liu, and N. E. Flower, *Physica C* **176**, 95 (1991).
 - ²³X. Zhao, X. Sun, X. Fan, W. Wu, X.-G. Li, S. Guo, and Z. Zhao, *Physica C* **307**, 265 (1998).
 - ²⁴T. Fujii, I. Terasaki, T. Watanabe, and A. Matsuda, *Phys. Rev. B* **66**, 024507 (2002).
 - ²⁵B. Liang, C. Bernhard, Th. Wolf, and C. T. Lin, *Supercond. Sci. Technol.* **17**, 731 (2004).
 - ²⁶A. Trokiner, L. Le Noc, J. Schneck, A. M. Pougnet, R. Mellet, J. Primot, H. Savary, Y. M. Gao, and S. Aubry, *Phys. Rev. B* **44**, 2426 (1991).
 - ²⁷S. A. Kivelson, *Physica B (Amsterdam)* **318**, 61 (2002).
 - ²⁸A. Schilling, H. R. Ott, and F. Hulliger, *Physica C* **157**, 144 (1989).
 - ²⁹M. Nideröst, A. Suter, P. Visani, A. C. Mota, and G. Blatter, *Phys. Rev. B* **53**, 9286 (1996).
 - ³⁰M. F. Goffman, J. A. Herbsommer, F. de la Cruz, T. W. Li, and P. H. Kes, *Phys. Rev. B* **57**, 3663 (1998).
 - ³¹A. Schilling, H. R. Ott, and Th. Wolf, *Phys. Rev. B* **46**, 14253 (1992).
 - ³²A. Piriou, Y. Fasano, E. Giannini, and Ø. Fischer, *Physica C* **460-462**, 408 (2007).
 - ³³G. Blatter, V. Geshkenbein, A. Larkin, and H. Nordborg, *Phys. Rev. B* **54**, 72 (1996).
 - ³⁴L. L. Daemen, L. N. Bulaevskii, M. P. Maley, and J. Y. Coulter, *Phys. Rev. Lett.* **70**, 1167 (1993).
 - ³⁵D. Ertaş and D. R. Nelson, *Physica C* **272**, 79 (1996); T. Giamarchi and P. Le Doussal, *Phys. Rev. B* **55**, 6577 (1997); V. Vinokur, B. Khaykovich, E. Zeldov, M. Konczykowski, R. A. Doyle, and P. Kes, *Physica C* **295**, 209 (1998); J. Kierfeld, *ibid.* **300**, 171 (1998).
 - ³⁶D. Giller, A. Shaulov, Y. Yeshurun, and J. Giapintzakis, *Phys. Rev. B* **60**, 106 (1999).
 - ³⁷V. Hardy, A. Wahl, A. Ruyter, A. Maignan, C. Martin, L. Coudrier, J. Provost, and Ch. Simon, *Physica C* **232**, 347 (1994); K. Shibata, T. Nishizaki, T. Sasaki, and N. Kobayashi, *Phys. Rev. B* **66**, 214518 (2002); T. Masui, Y. Takano, K. Yoshida, K. Kajita, and S. Tajima, *Physica C* **412-414**, 515 (2004).
 - ³⁸V. F. Correa, J. A. Herbsommer, E. E. Kaul, F. de la Cruz, and G. Nieva, *Phys. Rev. B* **63**, 092502 (2001).
 - ³⁹A. I. Larkin and Yu. N. Ovchinnikov, *J. Low Temp. Phys.* **34**, 409 (1979).
 - ⁴⁰C. P. Bean, *Rev. Mod. Phys.* **36**, 31 (1964).
 - ⁴¹N. Jenkins (private communication).
 - ⁴²M. Nideröst, R. Frassanito, M. Saalfrank, A. C. Mota, G. Blatter, V. N. Zavaritsky, T. W. Li, and P. H. Kes, *Phys. Rev. Lett.* **81**, 3231 (1998).
 - ⁴³D. Darminto, M. Diantoro, I. M. Sutjahja, A. A. Nugroho, W. Loeksmanto, and M. O. Tjia, *Physica C* **378-381**, 479 (2002).
 - ⁴⁴D. Darminto, M. O. Tjia, A. A. Nugroho, A. A. Menovsky, J. Shimoyama, and K. Kishio, *Physica C* **357-360**, 617 (2001).
 - ⁴⁵N. Musolino, N. Clayton, and R. Flükiger, *Physica C* **417**, 40

- (2004).
- ⁴⁶Y. Nakayama, T. Motohashi, K. Otschi, J. Shimoyama, K. Kitazawa, K. Kishio, M. Konczykowski, and N. Chikumoto, *Phys. Rev. B* **62**, 1452 (2000).
- ⁴⁷V. J. Emery and S. A. Kivelson, *Nature (London)* **374**, 434 (1995).
- ⁴⁸J. L. Tallon, C. Bernhard, U. Binniger, A. Hofer, G. V. M. Williams, E. J. Ansaldo, J. I. Budnick, and Ch. Niedermayer, *Phys. Rev. Lett.* **74**, 1008 (1995).
- ⁴⁹Ø. Fischer, M. Kugler, I. Maggio-Aprile, C. Berthod, and Ch. Renner, *Rev. Mod. Phys.* **79**, 353 (2007), and references therein.
- ⁵⁰N. Clayton, N. Musolino, E. Giannini, V. Garnier, and R. Flükiger, *Supercond. Sci. Technol.* **17**, S563 (2004).